Calcined palygorskite and smectite bearing marlstones as supplementary cementitious materials

Victor Poussardin, Michael Paris, William Wilson, Arezki Tagnit-Hamou, Dimitri Deneele

Calcined palygorskite and smectite bearing marlstones as supplementary cementitious materials

Victor Poussardin[1,2,3], Michael Paris[2], William Wilson[3], Arezki Tagnit-Hamou[3], Dimitri Deneele[1,2*]

[1]*GERS-GIE, Univ Gustave Eiffel, IFSTTAR, F-44344 Bouguenais, France*

[2]*Nantes Université, CNRS, Institut des Matériaux de Nantes Jean Rouxel, IMN, F-44000 Nantes, France*

[3]*Université de Sherbrooke, Sherbrooke, QC, Canada*

*corresponding author: dimitri.deneele@univ-eiffel.fr

Highlights

- Palygorskite-bearing marlstone is suitable for a use as a SCM
- Palygorskite-bearing marlstone exhibits a higher dihydroxylation (^{27}Al MAS NMR), self-reactivity in water and compressive strength in cementitious media than smectite-bearing marlstone.
- Pouzzolanic reactivity was significantly higher for systems with calcined palygorskite than calcined smectite only, as shown both by portlandite consumption (XRD) and C-(A)-S-H formation (^{29}Si MAS NMR).

Abstract

This article focuses on the use of two calcined marlstones as supplementary cementitious materials, one with palygorskite and smectite (MS1) as clay phases and the other with smectite only (MS2). The calcination and the reactivity of these two materials were first analysed by X-ray diffraction (XRD) and Magic Angle Spinning Solid State Nuclear Magnetic Resonance (MAS NMR). The two calcined marlstones were combined with Portland cement to produce mortars and measure compressive strength. The XRD and ^{27}Al MAS NMR results showed that 800°C is an optimal calcination temperature and that both calcined marlstones can be used as supplementary cementitious materials. The reactivity of MS1 was found to be higher than that of MS2. This was confirmed with compressive strength measurements which showed superior performance for mortars blended with calcined MS1 rather than calcined MS2. This difference between MS1 and MS2 is due to the presence of palygorskite in MS1, which greatly improves the reactivity and final mechanical performances. Therefore, palygorskite bearing marlstones are suitable for a use as SCM and this suggests that palygorskite exhibits a significant pozzolanic reactivity.

Keywords: Palygorskite, marlstone, SCMs, MAS NMR, calcined clay, dolomite

1. INTRODUCTION

In order to comply with the Paris climate agreements, and to limit the global temperature increase below 1.5°C compared to pre-industrial levels, the most polluting industrial sectors need to reduce significantly their greenhouse gas emissions (may their CO_2 emissions). It is estimated that 5 to 8% of global anthropogenic CO_2 emissions comes from the cement industry [1]. In this context, cement producers are seeking to reduce their carbon footprint.

The use of Supplementary Cementitious Materials (SCMs) to replace part of the clinker is now seen as one of the major solutions to reduce the environmental footprint of the cement industry [2]. Blast furnace slag [3, 4] and power plant fly ash [5–7] are the main examples of SCMs used today that reduce the environmental footprint of cement. However, blast furnace slag resources remain limited, preventing large-scale deployment of this technology, and fly ash reserves from coal combustion will continue to decline in the coming years as the energy transition legitimately limits their availability [2].

Among alternative SCMs, calcined clays are gaining in popularity. The resources of clays potentially viable as SCMs after calcination are abundant and well distributed around the world, especially in developing countries where the demand for cement is constantly growing [2]. The numerous studies carried out on the subject have shown that metakaolin (from the calcination of kaolin) has the highest reactivity in cementitious media [8–11], whereas calcined smectites [12–14] and illites [15–17] are much less reactive. These results led to a growing interest in the use of calcined kaolins (rock composed of kaolinite, quartz and minor accessory minerals) as SCMs, and to the development of Limestone Calcined Clay Cements (LC3) [18, 19].

Only few studies have looked at other types of clays than kaolinites, smectites and illites [20, 21], mainly because of industrial competition (which leads to higher prices) and lower availability. Furthermore, the majority of studies focused on relatively "pure" samples, which

are mainly composed of clay minerals, quartz and other accessory minor minerals. Yet it is common to find clay minerals associated with other compounds, especially carbonates. If the proportion of carbonates is high, this mixture of clay minerals and carbonates is named marlstone.

Marlstones are often neglected by manufacturers of fired clay materials such as bricks because of their high content of calcium carbonate. They are considered as waste by many industries and supplies are increasing [22]. However, these materials contain a significant proportion of clay minerals, which can become pozzolans upon calcination. The use of marlstones as SCMs could therefore make it possible to recover mining wastes (and/or overburdens) while reducing the environmental footprint of cement production. Numerous studies looked at the use of marlstones as SCMs [23–27] , but the great variability of this type of material limits the possibility of global analyses. For each type of marlstones considered as a potential SCM, it is imperative to understand the evolution of each phase (clay minerals and carbonates) composing the marlstones during its calcination, as well as its influence on the reactivity and the final mechanical performances of calcined marlstone-cement blends.

This study focuses on the use as SCMs of two marlstones considered as waste by the mining industry. The first objective is to determine whether these materials can be used as SCMs. The second objective is to study the physico-chemical changes taking place during the calcination and the reaction of these new pozzolans and to correlate this information with the final mechanical performances. The last objective is to determine how palygorskite (an unconventional clay contained in one of the two materials) contributes to the pozzolanic reactivity.

2. MATERIALS AND EXPERIMENTAL METHODS

2.1. Materials

The materials studied (MS1 and MS2) are two marlstones considered as waste by the mining industry. The samples were received as loose blocks and mechanically crushed before analysis.

Table 1 shows the results of the chemical analysis (performed by X-Ray Fluorescence (XRF). The proportions of each element are expressed in weight percent.

Table 1. Chemical analysis of MS1 and MS2.

	Element	O	Ca	Si	Mg	Al	Fe	K	P	Na	Ti	V
MS1	wt. %	55.5	**14.2**	**15.6**	**6.0**	**4.7**	1.5	1.0	0.6	0.2	0.2	0.1
MS2	wt. %	56.0	**16.4**	**16.2**	**5.5**	**3.8**	1.2	0.2	0.2	0.2	0.2	0

MS1 and MS2 have a very close chemical composition, especially regarding the proportions of silicon, calcium, magnesium and aluminium. These similarities in the chemistry of MS1 and MS2 are not surprising as both materials originate from the same sedimentary deposit.

X-ray diffraction analysis (XRD) was performed to highlight the mineralogical composition MS1 and MS2 and the different phases were quantified using the Rietveld refinement technique (see supporting information). Table 2 shows the results of the quantitative phases analysis for MS1 and MS2.

Table 2. wt.% of the crystalline phases of MS1 and MS2.

	Phase	Dolomite	Palygorskite	Smectite	Biotite	Hydroxylapatite	Quartz
MS1	wt.%	54	17	16	2	3	8
MS2	wt.%	59		27	1	2	11

MS1 and MS2 have a relatively close mineralogy, they are both mainly composed of dolomite associated with clay phases (smectite and biotite), quartz and hydroxylapatite. The main difference is the occurrence of palygorskite in MS1, which replaces part of the smectite.

2.2. Marlstone calcination

MS1 and MS2 were calcined at 600, 800 and 900°C in alumina crucibles using a laboratory furnace. The choice of these temperatures was made in accordance with the first study on calcination carried out on MS1 [28]. The materials were heated at a heating rate of 300°C/h and then maintained for 1 hour at maximum temperature. They were then left to cool until room temperature with the furnace door closed.

2.3. Hydration of calcined marlstones

The calcination and hydration of MS1 have already been the subject of two previous studies [29, 30] which demonstrated the formation of several reactive phases after calcination, notably CaO. As MS2 has a very close mineralogy to MS1, it is very likely to have the same reactive phases formed. Therefore, the pozzolanic activity of calcined MS1 and MS2 could not be measured using the classical pozzolanic activity tests (Chapelle test [31] and R^3 [32]), which requires the material tested not to contain free calcium. It was therefore decided to characterise the reactivity of these calcined materials by carrying out hydration tests.

For both MS1 and MS2, 1g of 800°C calcined material was manually mixed with water according to the chosen water to binder ratios (w/b = 0.8; 1; 2 and 4). The mixtures were left to react in sealed conditions for 7, 14, 28 and 180 days. At the end of each time period, the hydration was stopped by freezing at -24°C during 24h and freeze-drying during 48h under

vacuum. The dried materials were crushed and analysed by X-ray diffraction (XRD) and solid state nuclear magnetic resonance (MAS NMR). As the result analysis did not reveal any significant differences between the different w/b, only the hydration results for w/b = 0.8 are reported.

2.4. X-ray diffraction analysis (XRD)

Measurements were made with a Bruker D8 diffractometer using a Bragg-Brentano geometry with a copper anode tube X-ray source (40 kV/40 mA) emitting Cu Kα radiation. The acquisitions of the diffractograms were made between 4° and 60° 2θ with a step size of 0.017° 2θ and a measurement time of 1s per step. The Rietveld quantification of MS1 and MS2 was performed using the Profex Rietveld refinement program [33].

2.5. Solid state nuclear magnetic resonance (MAS NMR)

^{27}Al MAS NMR spectra were acquired in a 2.5 mm MAS probe using a Bruker Avance III 500 MHz spectrometer with the following parameters : MAS frequency of 30 kHz, excitation pulse length of $\pi/13$, radio frequency field of 11 kHz and repetition time of 1s.

^{29}Si MAS NMR spectra were acquired in a 7 mm MAS probe using a Bruker NEO 300 MHz spectrometer with the following parameters : MAS frequency of 5 kHz, excitation pulse length of $\pi/2$ and repetition time of 10s. The chosen 10s repetition time is too short to obtain a quantitative signal from the quartz, but as quartz is unreactive shorter repetition time can be used to save spectrometer time.

All the acquisitions were performed with ^{1}H decoupling. An aqueous solution of $Al(NO_3)_3$ was used to referenced ^{27}Al spectra while ^{29}Si spectra were referenced against TMS

(Tetramethylsilane). The Dmfit sotftware [34] was used to perform the spectral decompositions (see supporting information).

2.6. Calcined marlstone-cement blends and compressive strength measurements

The compressive strength was assessed on mortar cubes (50 x 50 x 50 mm^3) made with graded standard (supports ASTM C109) sand (sand to cement ratio = 2.75) and a constant water to binder ratio (w/b = 0.484). Blended cement was obtained by mixing 80 wt.% of general use Portland cement (GU) with 20 wt.% of 800°C calcined MS1 (for M-MS1 mortar) or MS2 (for M-MS2 mortar). The particle size distributions of the GU cement and MS1 and MS2 (before and after calcination) are shown in Table 3. The d-values indicate the maximal particle size diameter that includes 10% (d10), 50% (d50) and 90% (d90) of the particles (volume-weighted basis).

Table 3. Particle size distributions of GU cement and marlstones (MS1 and MS2) before and after calcination at 800°C.

Label	d10 (µm)	d50 (µm)	d90 (µm)
MS1	3.5	19.5	64.1
800°C-MS1	4.0	24.5	91.6
MS2	2.4	14.8	53.1
800°C-MS2	3.6	28.2	66.3
GU cement	3.5	20.5	59.7

Both 800°C-MS1 and 800°C-MS2 have a particle size distribution close to that of GU cement, which ensures homogeneous blends.

Control mortars cubes (labelled M-Ref) were prepared using 100% GU cement. A polycarboxylate (PC) superplasticizer (0.6% by total weight of binder) was used to obtain a flow equivalent to that of the control mixture (± 5 mm). Table 4 shows the proportions of the investigated mortars.

Table 4. Mix proportions of mortars

Label	Cement (g)	Pozzolan (g)	Sand (g)	Water (g)
M-Ref	500	0	1375	242
M-MS1	400	100	1375	242
M-MS2	400	100	1375	242

Mortars were mixed and specimens were molded according to the standard procedure ASTM C109 [35]. After molding, the specimens were placed in plastic bags for 20-24h until demolding. The demolded mortar cubes were stored in saturated lime water until testing. At 7 and 28 days the compressive strength was assessed according to the ASTM C109 loading procedure [35].

3. RESULTS AND DISCUSSION

3.1. Calcination

Fig. 1. displays the evolution of MS1 (Fig. 1.A) and MS2 (Fig. 1.B) X-ray diffractograms as a function of the calcination temperature.

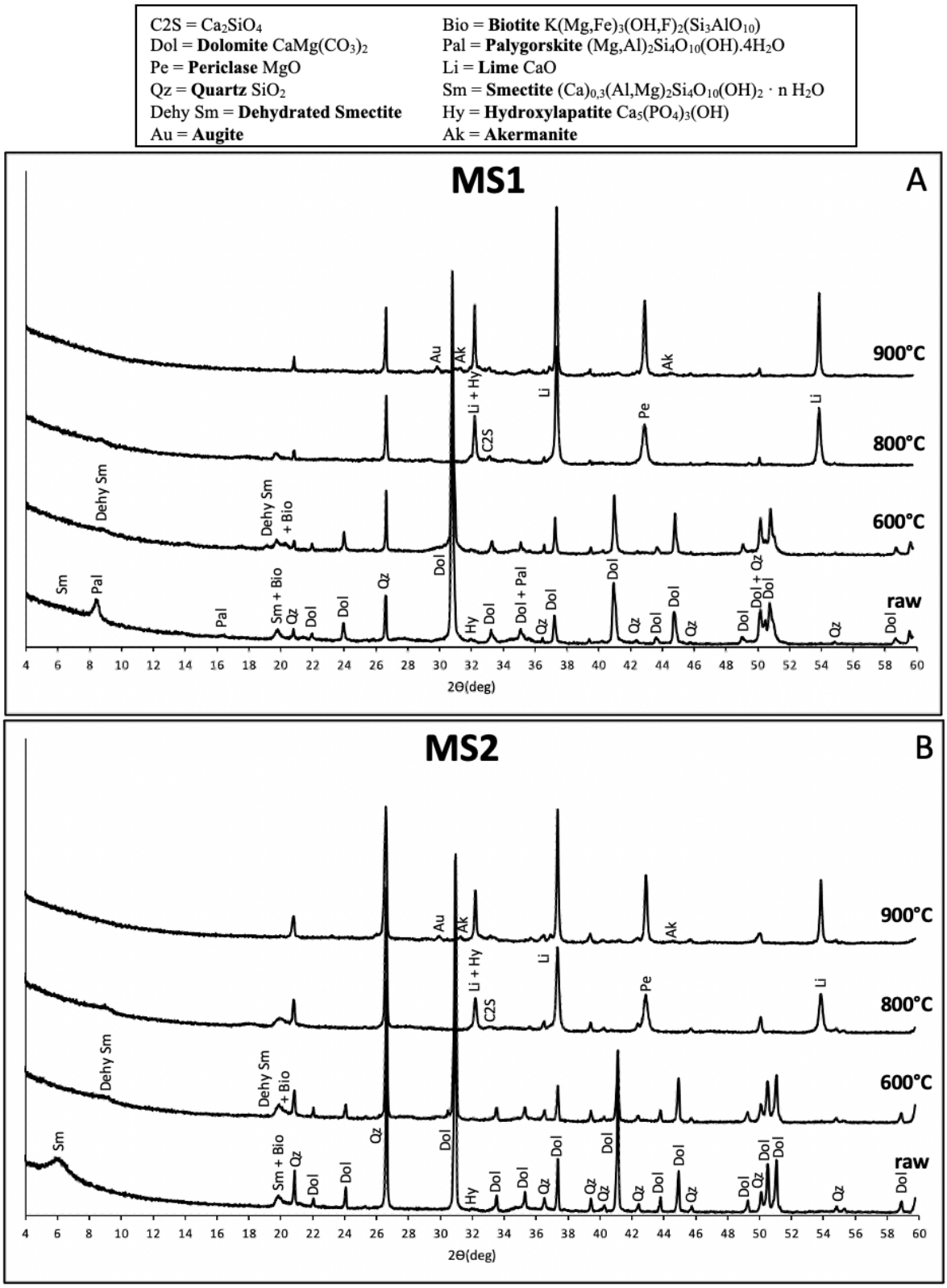

Fig. 1. Evolution of the X-ray diffractograms of MS1 (A) and MS2 (B) as a function of the calcination temperature.

At 600°C, for both MS1 and MS2 the 001 peak of smectite (Sm) is shifted from 6.2°(2θ) to 8.75°(2θ). This shift is explained by the dehydration of the smectite during the heat treatment (the removal of the interlayer water leads to a decrease in d001 basal spacing) [36, 37]. Concerning MS1, the characteristic peaks of palygorskite disappears at 600°C, reflecting its loss of crystallinity.

At 800°C, for both MS1 and MS2 the dolomite ($CaMg(CO_3)_2$) decarbonates into lime (CaO) and periclase (MgO) and a peak associated with dicalcium silicate (C_2S) appears. However, the low intensity of the C_2S peaks (possibly due to low crystallinity of the phase) hinders the determination of the type of polymorph. The fact that this C_2S is formed at the same temperature as the lime supports the hypothesis that it results from a recombination phenomenon between the calcium from the decarbonated dolomite and the silicon from calcined clay phases [38].

At 900°C, for both MS1 and MS2 the characteristic peaks of dehydrated smectite and biotite disappear, indicating a complete loss of crystallinity of these two phyllosilicates. Quartz and hydroxylapatite are not sensitive to heat treatment since their peaks remain detectable up to 900°C. Finally, there are recrystallisation phenomena in the form of augite and akermanite at 900°C.

Based on these XRD results, 800°C seems to be a suitable calcination temperature as it allows the loss of crystallinity of the clay phases without causing recrystallisation phenomena (that could reduce the reactivity) for both MS1 and MS2.

Fig. 2. displays the evolution of the ^{27}Al MAS NMR spectra of MS1 (Fig. 2.A) and MS2 (Fig. 2.B) as a function of the calcination temperature.

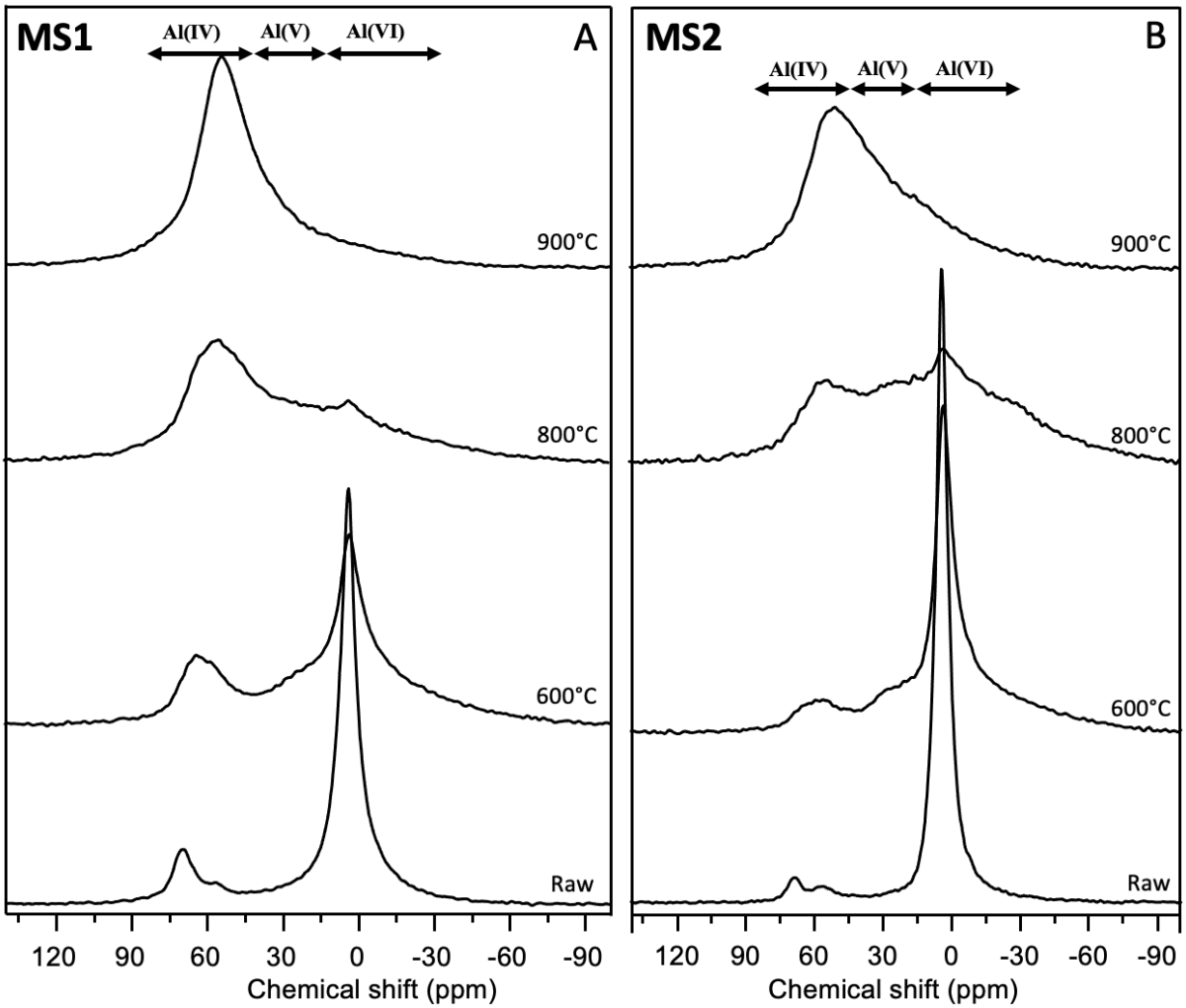

Fig. 2. Evolution of the ^{27}Al MAS NMR spectra of MS1 (A) and MS2 (B) as function of the calcination temperature.

Both spectra of raw MS1 and MS2 exhibit two main resonances at 3 and 70 ppm which correspond to 6-fold and 4-fold aluminium, respectively [39]. The 6-fold aluminium resonance (3 ppm) can be associated with aluminium in palygorskite, smectite and biotite for MS1 and with aluminium in smectite and biotite for MS2 [40]. The 4-fold aluminium resonance (70 ppm) can be associated with the isomorphic substitution of silicon by aluminium atoms into silicate layers of palygorskite, smectite and biotite structures for MS1 and into smectite and biotite

structures for MS2 [40]. A weak resonance at 57 ppm is detected in both MS1 and MS2 spectra, which corresponds to aluminium in q4(4Si) configuration [41] possibly associated with an additional phase occurring in low quantity and/or with low crystallinity, undetectable by XRD.

With the increasing calcination temperature, the 6-fold aluminium resonance intensity decreases while two new resonances appear at 27 and 59 ppm, which correspond to 5-fold and 4-fold aluminium, respectively [39]. During the calcination of MS1 and MS2, the calcination leads to a departure of hydroxyl groups from the clay phases (the dehydroxylation phenomenon). The octahedral (6-fold) aluminium atoms to which these hydroxyl groups were bonded have changed their coordination to 5- and 4-fold aluminium atoms. The pozzolanic activity of a calcined clay could be directly related to the relative proportion of 5- and 4-fold aluminium. These sites, in particular at the 5-fold one, are the starting point of the dissolution and the initiation of the pozzolanic reaction [15]. For both MS1 and MS2, the highest relative proportion of aluminium 5 and 4 (without recrystallization) is reached at 800°C, which suggests that this calcination temperature should allow the highest pozzolanic reactivity. By comparing the evolution of MS1 and MS2 it is clear that the dehydroxylation occurs more easily in MS1 (which contains smectite and palygorskite) than in MS2 (which contains only smectite). At 800°C, a significantly higher relative proportion of 6-fold aluminium is still remaining in MS2 than in MS1. This difference can be explained by the occurrence of palygorskite in MS1, which was found to dehydroxylate more efficiently (at lower temperature) than smectite and biotite.

Fig. 3. displays the evolution of the ^{29}Si MAS NMR spectra of MS1 (Fig. 3.A) and MS2 (Fig. 3.B) as a function of the calcination temperature.

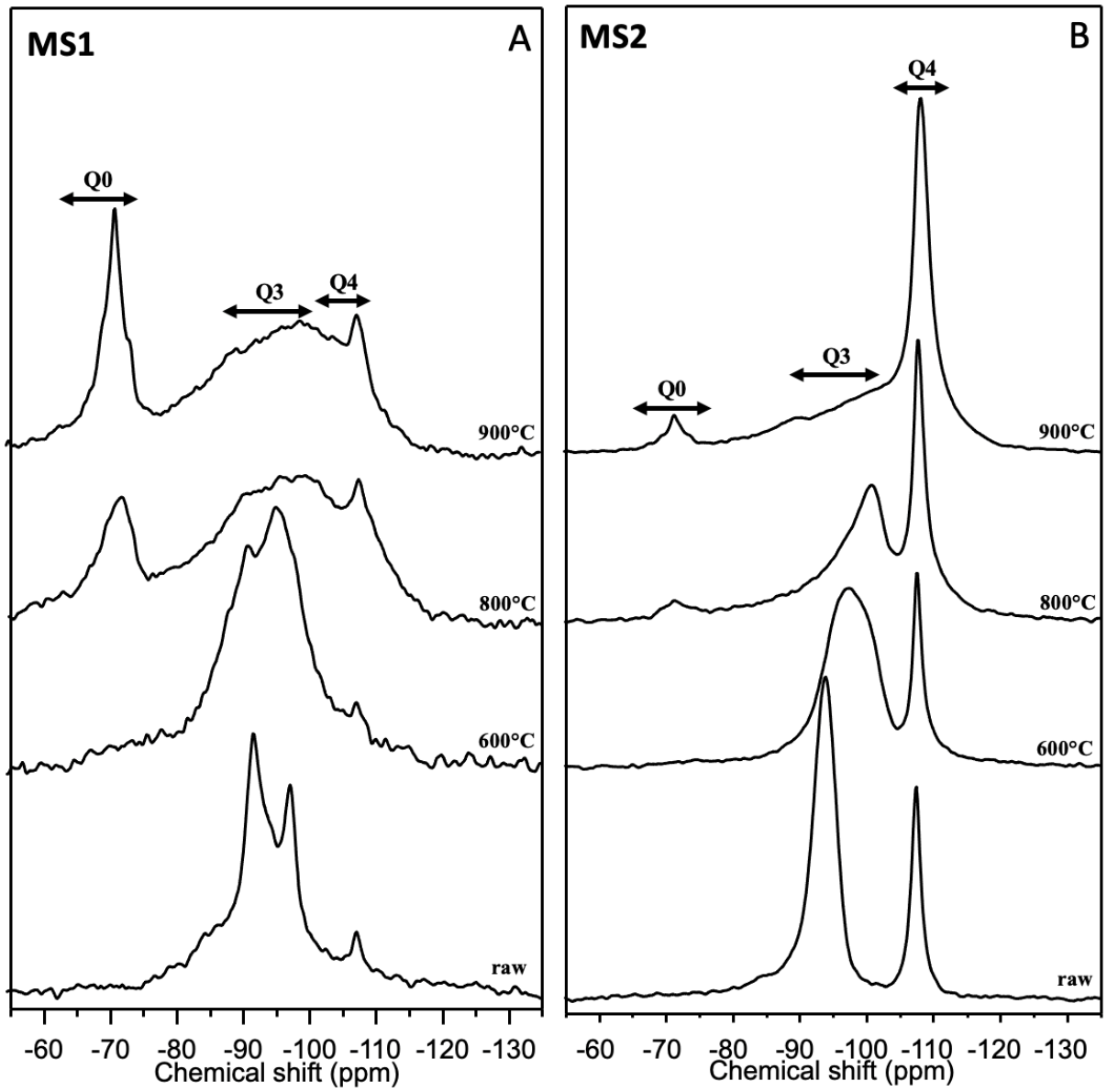

Fig. 3. Evolution of the ^{29}Si MAS NMR spectra of MS1 (A) and MS2 (B) as function of the calcination temperature.

Both spectra of raw MS1 and MS2 exhibit a resonance at -108 ppm which correspond to Q^4 silicon atoms and which can be associated with silicon in the quartz structure [42]. For MS1, the total signal between -84 and -100 ppm is composed of Q^3 silicon atoms of smectite (-93 ppm) [12], Q^3(1Al) silicon atoms of biotite (-86 ppm) [43], Q^2 silicon atoms of palygorskite (-

84 ppm) [44] and two Q^3 silicon sites of palygorskite at -98 and -92 ppm which correspond to SiO_4 at the edges and at the centre of the ribbons of tetrahedra, respectively [45]. For MS2, the total signal is only composed of Q^3 silicon atoms of smectite and Q^3(1Al) silicon atoms of biotite and smectite. For both MS1 and MS2, the increase of the calcination temperature leads to a broadening of the resonances associated with the Q^3 of the clay phases. This broadening is explained by a distribution of the environments of the silicon atoms and indicate a structural loss of the clay phases upon calcination [46]. At 800°C a new resonance appears at -71 ppm in MS1 and MS2 spectra. This new resonance corresponds to Q^0 silicon atoms and can be associated with the silicon contained in the C_2S structure [47], in accordance with XRD results. With increasing the calcination temperature there is a low-frequency shift of the Q^3 resonances for MS2, which is explained by the condensation of the Q^3 into Q^4 silica [17]. By comparing MS1 and MS2 it is evident that the C_2S formation is facilitated in MS1 compared to MS2 (a higher relative proportion is observed). This could be explained by the occurrence of palygorskite as it is the only main difference between both materials. However, this difference of C_2S formation between MS1 and MS2 is not observable by XRD, meaning that the main part of this C_2S is amorphous.

Overall, the results of XRD and MAS NMR indicates that 800°C is probably the best calcination temperature for both MS1 and MS2. Moreover, MS1 seems to be more sensitive to the calcination, which leads to higher dehydroxylation of the clay phases and to higher relative amount of C_2S. The major difference between MS1 and MS2 being the occurrence of palygorskite in MS1, it seems clear that smectite and palygorskite have different responses to calcination.

3.2. Self-reactivity of calcined marlstones in water

The calcination study of MS1 and MS2 revealed the formation of different reactive phases such as lime, periclase and C_2S as well as the loss of crystallinity of the clay phases. MS1 and MS2 were thus hydrated in water in order to study their reactivity, the contribution of each phases, their evolution and the possible presence of synergies.

Fig. 4. displays the evolution of the X-ray diffractograms of MS1 (Fig. 4.A) and MS2 (Fig. 4.B) calcined at 800°C and hydrated in water for 7, 14, 28 and 180 days.

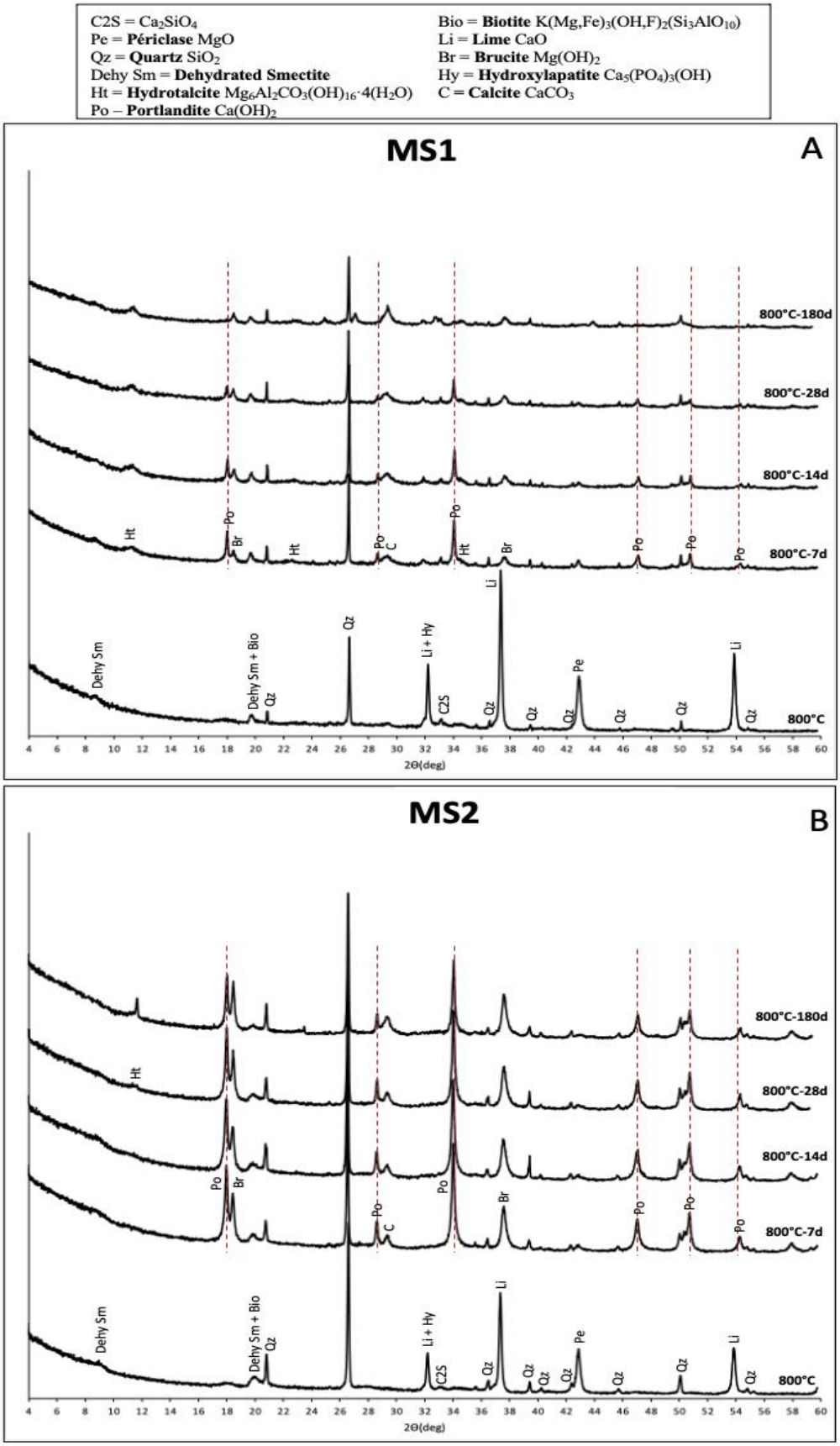

Fig. 4. Evolution of the X-ray diffractograms of MS1 (A) and MS2 (B) calcined at 800°C and hydrated (w/b = 0.8) during 7, 14, 28 and 180 days.

After 7 days of hydration, for both MS1 and MS2, diffraction peaks characteristic of portlandite, calcite, hydrotalcite and brucite appear on the diffractograms. The formation of portlandite comes from the hydration of lime and calcite comes from its carbonation. The magnesium from the periclase is incorporated into two phases: brucite and hydrotalcite.

The formation of brucite can be problematic in cements. The hydration of periclase into brucite is a phenomenon that has relatively long kinetic compared to the hardening kinetic of cement. This post-hardening swelling can lead to cracking problems and therefore a loss of mechanical performance if there is not enough space available in the matrix [48]. Studies are currently underway to determine whether neoformed brucite leads to cracking in this system. However, there is no post-hardening swelling phenomenon associated with hydrotalcite (the second magnesian phase neoformed in our system) formation in the existing literature and the possible existence of synergies with the cement phases could enhance the formation of hydrotalcite instead of brucite in calcined marlstone-cement system.

The amount of neoformed brucite and portlandite is higher for MS2 than for MS1 (larger area under the peaks), therefore it is difficult to compare the evolution of these two phases between MS1 and MS2. With the increasing hydration time, the intensity of the peaks characteristic of portlandite decrease for MS1 and MS2. However, after 180 days of hydration the portlandite diffraction peaks are no longer detectable in MS1. This total consumption of portlandite in MS1 could be a first indication of a possible stronger pozzolanic reactivity compared to MS2. However, this apparent consumption of portlandite may also be due to its carbonation into calcite as we observe an increase in the intensity of the peak associated with calcite with increasing hydration time.

Fig. 5. shows the evolution of the ^{29}Si MAS NMR spectra of MS1 (Fig. 5.A) and MS2 (Fig. 5.B) calcined at 800°C and hydrated in water during 7, 14, 28 and 180 days.

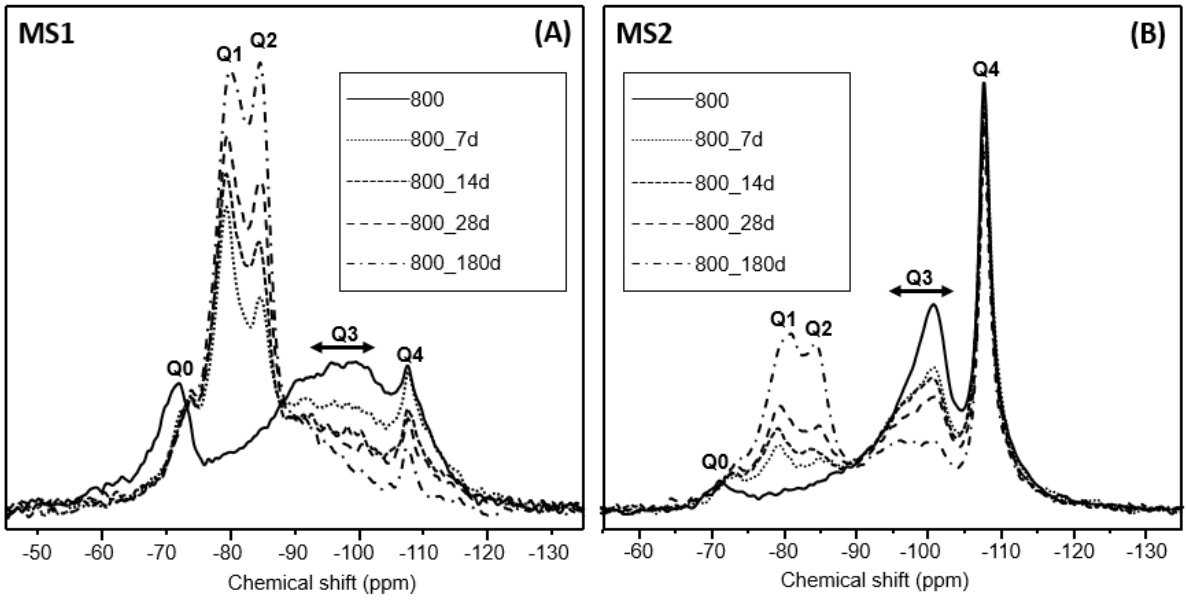

Fig. 5. Evolution of the ^{29}Si MAS NMR spectra of MS1 (A) and MS2 (B) calcined at 800°C and hydrated (w/b = 0.8) during 7, 14, 28 and 180 days.

After 7 days of hydration for both MS1 and MS2, a decrease is observed for the intensity of the broad Q^3 resonances previously associated with the calcined clay phases. This decrease is correlated with the appearance of two new resonances at -78 and -85 ppm which correspond to Q^1 and Q^2 silicon atoms, respectively [49]. Q^1 silicon atoms can be associated with pairs of linked silicate tetrahedral (dimers) and/or terminal tetrahedral silicate groups of C-S-H. Q^2 silicon atoms can be associated with C-S-H tetrahedral silicate groups in bridging (Q^2-B) and/or intermediates (Q^2-P) configurations [50].

The -71 ppm resonance corresponding to Q^0 atoms (associated previously with C_2S neoformed during calcination) decreases considerably after 7 days of hydration and leaves a resonance at -73 ppm for both MS1 and MS2. This -73 ppm resonance can either be associated with the Q^1 atoms of akermanite/gehlenite and/or Q^0 of non-reactive C_2S. The fact that the C_2S XRD signal remains detectable even after 180 days of hydration supports the hypothesis that some of the C_2S is non-reactive (the crystallised one). However, during the calcination of MS1 and MS2, the formation of akermanite was observed at 900°C (Fig. 1.). The -73 ppm signal can thus also

be associated with akermanite which is not yet crystallised enough to be detectable by XRD at 800°C. Finally, several studies have highlighted the formation of gehlenite during the calcination of marlstones [51, 52] and this signal at -73 ppm could therefore be associated with this phase.

After 14 days of hydration, for both MS1 and MS2, the intensity of the Q^3 calcined clay phases resonances continues to decrease while the intensity of the Q^1 + Q^2 resonances associated with C-S-H increases. A new resonance at -81 ppm appears after 14 days for MS1 and 28 days for MS2, which corresponds to silicon in Q^2(1Al) configuration and confirms the incorporation of aluminium into the C-A-S-H structure, which is characteristic of the pozzolanic reaction of calcined clays. The trend will continue up to 180 days for MS1 and MS2, validating the intrinsic pozzolanic reactivity of these two calcined materials.

The comparison of the series of spectra indicates that the formation of C-A-S-H and the consumption of calcined clay phases are significantly higher for MS1 than MS2. Spectral integration quantification was thus carried out to precisely compare the difference between MS1 and MS2 in terms of the consumption of calcined clay phases and the formation of C-A-S-H.

Fig. 6. displays the evolution of the relative proportions (from the perspective of silicon content) of the Qn (C-A-S-H) and the Q^3 (calcined clay phases) for hydrated 800°C-MS1 (Fig 6.A) and 800°C-MS2 (Fig 6.B). Details of this quantification by spectral integration are given in the supporting information. The Q^4 signal associated with quartz is not quantitative and the Q^0-Q^1 signal associated with C_2S and/or akermanite/gehlenite is constant from 7 days and onward. Therefore, Fig 6. includes only the evolution of the Q^3 (and Q^3-Q^4 for MS2) of the calcined clay phases and Q^n of the C-A-S-H.

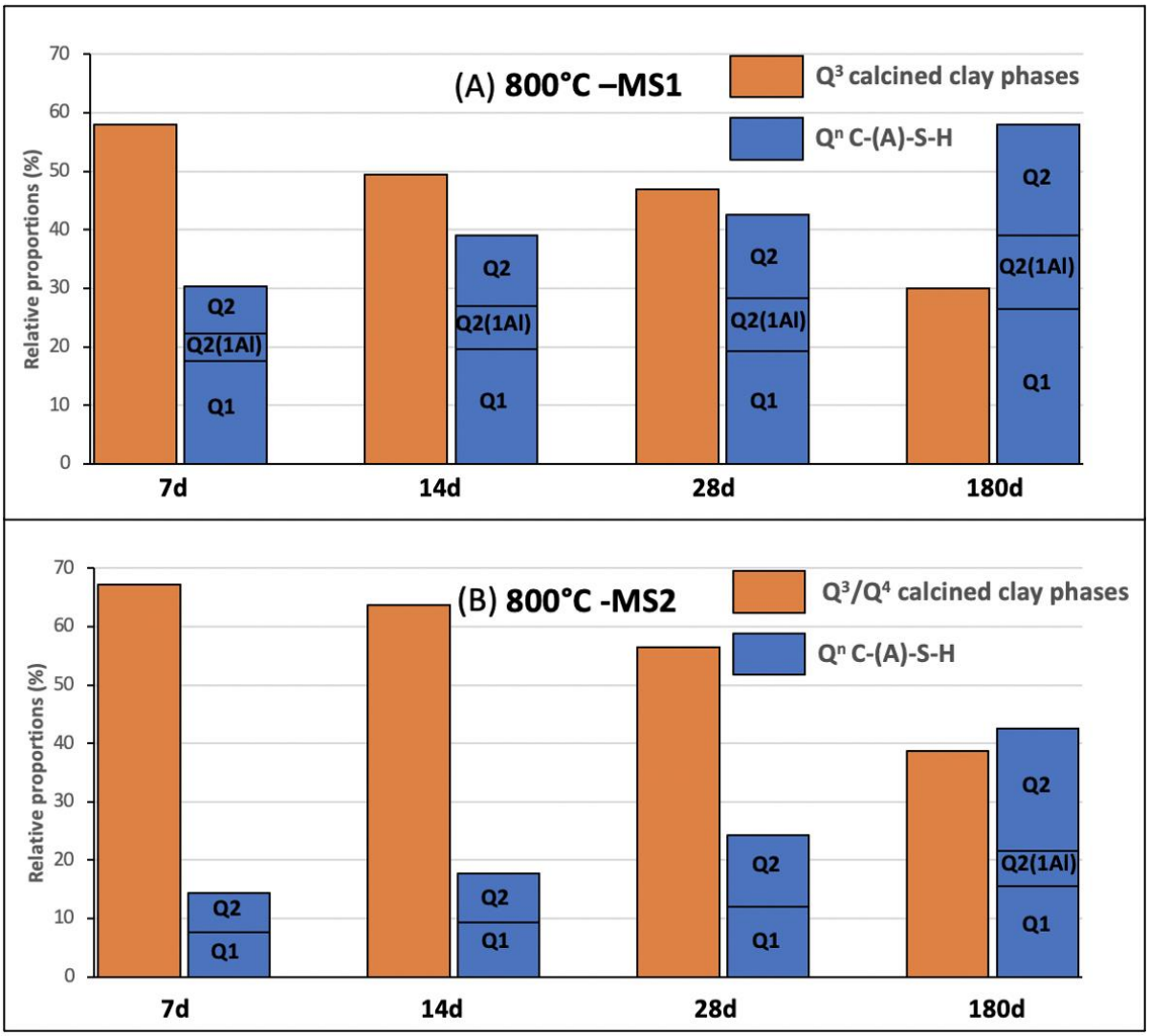

Fig. 6. Relative proportions of silicon-containing phases of MS1 (A) and MS2 (B) calcined at 800°C (from the perspective of silicon content) as function of the hydration time obtained from ^{29}Si MAS NMR spectra.

For MS1, after only 7 days of hydration, the relative proportion of silicon in Q^n configuration associated with C-A-S-H is already 30%. From 7 to 180 days of hydration, the relative proportion of silicon in Q^3 configuration associated with the calcined clay phases decreases from 58% to 30%. In parallel, the relative proportion of Q^1, Q^2(1Al) and Q^2 silicon associated with the C-(A)-S-H increases from 30% to 58%.

For MS2, after 7 days of hydration, the relative proportion of silicon in Qn configuration associated with C-A-S-H is only 14%, which is much lower than for MS1 (30%). From 7 to

180 days of hydration the relative proportion of silicon in Q^3-Q^4 configuration associated with the calcined clay phases decreases from 67% to 39%. In parallel, the relative proportion Q^1, Q^2(1Al) and Q^2 silicon associated with the C-(A)-S-H increases from 14% to 43%. The consumption of the calcined clay phases, associated with the formation of C-A-S-H and the consumption of portlandite during hydration confirms the pozzolanic reactivity of MS1 and MS2 calcined at 800°C. However, this pozzolanic reactivity is more important for MS1 (which contains palygorskite) than for MS2 ($\frac{Q^n\ (CASH)}{Q^3}$ = 1,93 for MS1 and $\frac{Q^n\ (CASH)}{Q^3+Q^4}$ = 1,13 for MS2 after 180 days of hydration). Compressive strengths were measured on mortars incorporating the two marlstones calcined at 800°C to confirm their different reactivity.

3.3. Calcined marlstone-cement blends

Fig. 7. displays the compressive strength of M-Ref, M-MS1 and M-MS2 after 7 and 28 days of hydration. The error bars indicate the standard deviation for each set of 3 compression measurements.

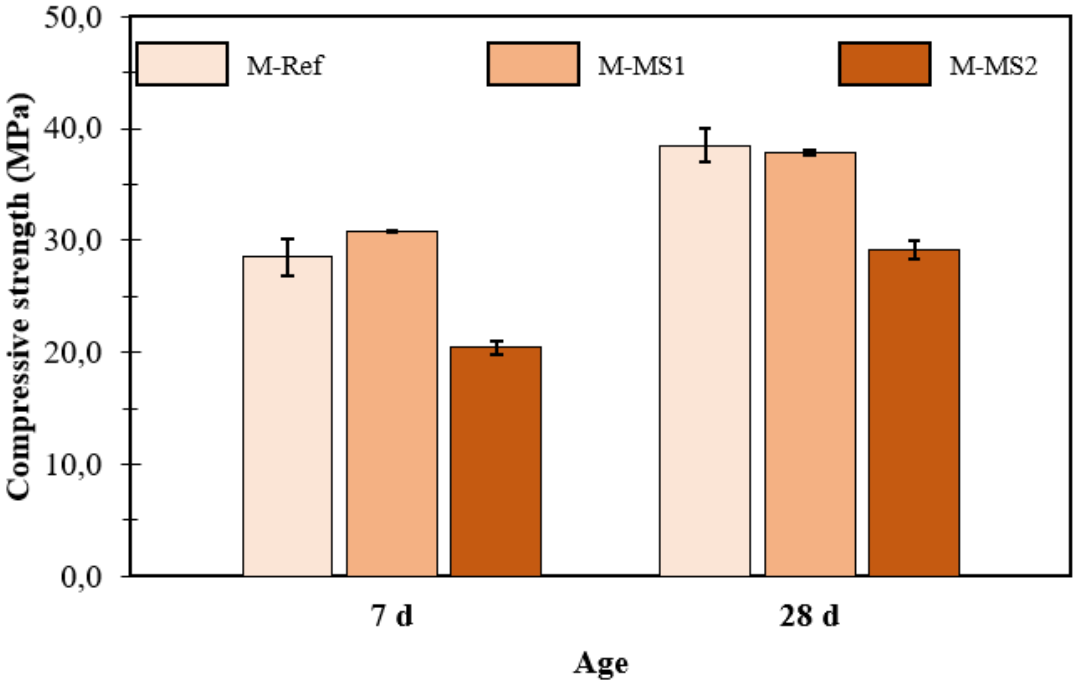

Fig. 7. Compressive strengths at 7 and 28 days of M-Ref, M-MS1 and M-MS2

After 7 days M-MS1 shows a compressive strength slightly higher (31 MPa) to that of the reference (29 MPa for M-ref) whereas M-MS2 shows a significant lower strength (20 MPa). At 28 days the trend continues for M-MS1 which shows an equivalent compressive strength (38 MPa) to that of the reference (39 MPa) whereas M-MS2 still shows significant lower compressive strength (29 MPa).

The better mechanical performance of M-MS1 confirms the previous results assessed by ^{27}Al and ^{29}Si MAS NMR. The occurrence of palygorskite in MS1 leads to a higher degree of dehydroxylation at 800°C in comparison to MS2 (Fig. 2.). This enhances the pozzolanic reactivity of 800°C-MS1 in comparison to 800°C-MS2 (Fig. 6.) and results in higher compressive strengths at 7 and 28 days (Fig. 7.). These results suggest that the palygorskite has a higher pozzolanic activity after calcination at 800°C than smectite. To a lesser extent, the higher mechanical performance of M-MS1 compared to M-MS2 could also be attributed to the greater amount of C_2S neoformed during the calcination (facilitated by the occurrence of palygorskite).

CONCLUSION

This paper compares the use of two calcined marlstones as SCMs in terms of calcination, self-reactivity in water and mechanical performance in cementitious blends. The two marlstones differ mainly by the presence of palygorskite (MS1) or not (MS2). Based on the results presented, the following conclusions can be drawn:

1. The calcination of MS1 and MS2 leads to the dehydroxylation of the clay phases associated with the formation of lime, periclase and C_2S. A calcination temperature of 800°C resulted in the highest expected reactivity for both MS1 and MS2. The degree of dehydroxylation and the

amount of C_2S neoformed are higher for MS1 than MS2, which was attributed to the occurence of palygorskite in MS1.

2. Both MS1 and MS2 calcined at 800°C exhibit significant self-reactivity in water, mainly pozzolanic. The comparative study shows that MS1 calcined at 800°C exhibits a higher self-reactivity than MS2 confirming the results of the calcination analysis.

3. The comparative study shows that mortars made from cement blended with 20% of MS1 calcined at 800°C have much better compressive strength than those made with MS2 after 7 and 28 days. Once again, this confirms the results of the calcination (higher dehydroxylation of MS1 than MS2) and self-reactivity in water analysis (higher reactivity of 800°C-MS1 than 800°C-MS2).

4. Calcination, self-reactivity in water and compressive strength results indicate that calcined palygorskite-bearing marlstones have higher potential use as SCMs in cementitious systems than calcined smectite-bearing marlstones. These results open up new applications for this type of marlstones and suggest that palygorskite is a clay that could be used as SCM once calcined.

REFERENCES

1. Huntzinger DN, Eatmon TD (2009) A life-cycle assessment of Portland cement manufacturing: comparing the traditional process with alternative technologies. Journal of Cleaner Production 17:668–675. https://doi.org/10.1016/j.jclepro.2008.04.007

2. Scrivener KL, John VM, Gartner EM (2018) Eco-efficient cements: Potential economically viable solutions for a low-CO2 cement-based materials industry. Cement and Concrete Research 114:2–26. https://doi.org/10.1016/j.cemconres.2018.03.015

3. Escalante JI, Gómez LY, Johal KK, et al (2001) Reactivity of blast-furnace slag in Portland cement blends hydrated under different conditions. Cement and Concrete Research 31:1403–1409. https://doi.org/10.1016/S0008-8846(01)00587-7

4. Yazıcı H, Yardımcı MY, Yiğiter H, et al (2010) Mechanical properties of reactive powder concrete containing high volumes of ground granulated blast furnace slag. Cement and Concrete Composites 32:639–648. https://doi.org/10.1016/j.cemconcomp.2010.07.005

5. Sakai E, Miyahara S, Ohsawa S, et al (2005) Hydration of fly ash cement. Cement and Concrete Research 35:1135–1140. https://doi.org/10.1016/j.cemconres.2004.09.008

6. Yao ZT, Ji XS, Sarker PK, et al (2015) A comprehensive review on the applications of coal fly ash. Earth-Science Reviews 141:105–121. https://doi.org/10.1016/j.earscirev.2014.11.016

7. Hu X, Shi C, Shi Z, Zhang L (2019) Compressive strength, pore structure and chloride transport properties of alkali-activated slag/fly ash mortars. Cement and Concrete Composites 104:103392. https://doi.org/10.1016/j.cemconcomp.2019.103392

8. Alujas A, Fernández R, Quintana R, et al (2015) Pozzolanic reactivity of low grade kaolinitic clays: Influence of calcination temperature and impact of calcination products on OPC hydration. Applied Clay Science 108:94–101. https://doi.org/10.1016/j.clay.2015.01.028

9. Almenares RS, Vizcaíno LM, Damas S, et al (2017) Industrial calcination of kaolinitic clays to make reactive pozzolans. Case Studies in Construction Materials 6:225–232. https://doi.org/10.1016/j.cscm.2017.03.005

10. El-Diadamony H, Amer AA, Sokkary TM, El-Hoseny S (2018) Hydration and characteristics of metakaolin pozzolanic cement pastes. HBRC Journal 14:150–158. https://doi.org/10.1016/j.hbrcj.2015.05.005

11. Zhao D, Khoshnazar R (2020) Microstructure of cement paste incorporating high volume of low-grade metakaolin. Cement and Concrete Composites 106:103453. https://doi.org/10.1016/j.cemconcomp.2019.103453

12. Brown IW, MacKenzie KJD, Meinhold RH (1987) The thermal reactions of montmorillonite studied by high-resolution solide-state 29Si and 27Al NMR

13. Garg N, Skibsted J (2014) Thermal Activation of a Pure Montmorillonite Clay and Its Reactivity in Cementitious Systems. The Journal of Physical Chemistry C 118:11464–11477. https://doi.org/10.1021/jp502529d

14. Kaminskas R, Kubiliute R, Prialgauskaite B (2020) Smectite clay waste as an additive for Portland cement. Cement and Concrete Composites 113:103710. https://doi.org/10.1016/j.cemconcomp.2020.103710

15. Fernandez R, Martirena F, Scrivener KL (2011) The origin of the pozzolanic activity of calcined clay minerals: A comparison between kaolinite, illite and montmorillonite. Cement and Concrete Research 41:113–122. https://doi.org/10.1016/j.cemconres.2010.09.013

16. Taylor-Lange SC, Rajabali F, Holsomback NA, et al (2014) The effect of zinc oxide additions on the performance of calcined sodium montmorillonite and illite shale supplementary cementitious materials. Cement and Concrete Composites 53:127–135. https://doi.org/10.1016/j.cemconcomp.2014.06.008

17. Garg N, Skibsted J (2016) Pozzolanic reactivity of a calcined interstratified illite/smectite (70/30) clay. Cement and Concrete Research 79:101–111. https://doi.org/10.1016/j.cemconres.2015.08.006

18. Cancio Díaz Y, Sánchez Berriel S, Heierli U, et al (2017) Limestone calcined clay cement as a low-carbon solution to meet expanding cement demand in emerging economies. Development Engineering 2:82–91. https://doi.org/10.1016/j.deveng.2017.06.001

19. Scrivener K, Martirena F, Bishnoi S, Maity S (2018) Calcined clay limestone cements (LC3). Cement and Concrete Research 114:49–56. https://doi.org/10.1016/j.cemconres.2017.08.017

20. He C, Makovicky E, Osbæck B (1996) Thermal treatment and pozzolanic activity of sepiolite. Applied Clay Science 10:337–349. https://doi.org/10.1016/0169-1317(95)00035-6

21. He C, Osbaeck B, Makovicky E (1995) Pozzolanic reactions of six principal clay minerals: Activation, reactivity assessments and technological effects. Cement and Concrete Research 25:1691–1702. https://doi.org/10.1016/0008-8846(95)00165-4

22. Justnes H, Østnor T, De Weerdt K, Vikan H (2021) CALCINED MARL AND CLAY AS MINERAL ADDITION FOR MORE SUSTAINABLE CONCRETE STRUCTURES CALCINED MARL AND CLAY AS MINERAL ADDITION FOR MORE SUSTAINABLE CONCRETE STRUCTURES

23. Danner T, Norden G, Justnes H (2018) Characterisation of calcined raw clays suitable as supplementary cementitious materials. Applied Clay Science 162:391–402. https://doi.org/10.1016/j.clay.2018.06.030

24. Bullerjahn F, Zajac M, Pekarkova J, Nied D (2020) Novel SCM produced by the co-calcination of aluminosilicates with dolomite. Cement and Concrete Research 134:106083. https://doi.org/10.1016/j.cemconres.2020.106083

25. Mohammed S, Elhem G, Mekki B (2016) Valorization of pozzolanicity of Algerian clay: Optimization of the heat treatment and mechanical characteristics of the involved cement mortars. Applied Clay Science 132–133:711–721. https://doi.org/10.1016/j.clay.2016.08.027

26. Danner T, Norden G, Justnes H (2021) Calcareous smectite clay as a pozzolanic alternative to kaolin. European Journal of Environmental and Civil Engineering 25:1647–1664. https://doi.org/10.1080/19648189.2019.1590741

27. Bahhou A, Taha Y, Khessaimi YE, et al (2021) Using Calcined Marls as Non-Common Supplementary Cementitious Materials—A Critical Review. Minerals 11:517. https://doi.org/10.3390/min11050517

28. Poussardin V, Wilson W, Paris M, et al Calcined palygorskites as supplementary cementitious materials

29. Poussardin V, Paris M, Tagnit-Hamou A, Deneele D (2020) Potential for calcination of a palygorskite-bearing argillaceous carbonate. Applied Clay Science 198:105846. https://doi.org/10.1016/j.clay.2020.105846

30. Poussardin V, Paris M, Wilson W, et al (2022) Self-reactivity of a calcined palygorskite-bearing marlstone for potential use as supplementary cementitious material. Applied Clay Science 216:106372. https://doi.org/10.1016/j.clay.2021.106372

31. Ferraz E, Andrejkovičová S, Hajjaji W, et al (2015) Pozzolanic activity of metakaolins by the French standard of the modified Chapelle test: A direct methology. Acta Geodynamica et Geomaterialia 12:289–298. https://doi.org/10.13168/AGG.2015.0026

32. Avet F, Snellings R, Alujas Diaz A, et al (2016) Development of a new rapid, relevant and reliable (R3) test method to evaluate the pozzolanic reactivity of calcined kaolinitic clays. Cement and Concrete Research 85:1–11. https://doi.org/10.1016/j.cemconres.2016.02.015

33. Doebelin N, Kleeberg R (2015) *Profex* : a graphical user interface for the Rietveld refinement program *BGMN*. Journal of Applied Crystallography 48:1573–1580. https://doi.org/10.1107/S1600576715014685

34. Massiot D, Fayon F, Capron M, et al (2002) Modelling one- and two-dimensional solid-state NMR spectra: Modelling 1D and 2D solid-state NMR spectra. Magn Reson Chem 40:70–76.

https://doi.org/10.1002/mrc.984

35. C01 Committee Test Method for Compressive Strength of Hydraulic Cement Mortars (Using 2-in. or [50-mm] Cube Specimens). ASTM International

36. Bala P, Samantaray BK, Srivastava SK (2000) Dehydration transformation in Ca-montmorillonite. Bulletin of Materials Science 23:61–67. https://doi.org/10.1007/BF02708614

37. Morodome S, Kawamura K (2009) Swelling Behavior of Na- and Ca-Montmorillonite up to 150°C by in situ X-ray Diffraction Experiments. Clays and Clay Minerals 57:150–160. https://doi.org/10.1346/CCMN.2009.0570202

38. Xie J, Chen T, Xing B, et al (2016) The thermochemical activity of dolomite occurred in dolomite–palygorskite. Applied Clay Science 119:42–48. https://doi.org/10.1016/j.clay.2015.07.014

39. Maia AÁB, Angélica RS, de Freitas Neves R, et al (2014) Use of 29Si and 27Al MAS NMR to study thermal activation of kaolinites from Brazilian Amazon kaolin wastes. Applied Clay Science 87:189–196. https://doi.org/10.1016/j.clay.2013.10.028

40. Sanz J, Serratosa JM (1984) Silicon-29 and aluminum-27 high-resolution MAS-NMR spectra of phyllosilicates. Journal of the American Chemical Society 106:4790–4793. https://doi.org/10.1021/ja00329a024

41. Muller D, Gessner W, Samoson A, Lippmaa E (1986) Solid-state Aluminium-27 Nuclear Magnetic Resonance Chemical Shift and Quadrupole Coupling Data for Condensed AIO4, Tetrahedra. J Chem Soc Dalton Trans 5

42. Lippmaa E, Maegi M, Samoson A, et al (1980) Structural studies of silicates by solid-state high-resolution silicon-29 NMR. Journal of the American Chemical Society 102:4889–4893. https://doi.org/10.1021/ja00535a008

43. Mackenzie KJD, Brown IWM, Cardile CM, Meinhold RH (1987) The thermal reactions of muscovite studied by high-resolution solid-state 29-Si and 27-Al NMR. Journal of Materials Science 22:2645–2654. https://doi.org/10.1007/BF01082158

44. Kuang W, Facey GA, Detellier C (2004) Dehydration and rehydration of palygorskite and the influence of water on the nanopores. Clays Clay Miner 52:635–642. https://doi.org/10.1346/CCMN.2004.0520509

45. Barron PF, Frost RL, Qlil N (1985) Solid state 29Si NMR examination of the 2:1 ribbon magnesium silicates, sepiolite and palygorskite. American Mineralogist 70:758–766

46. MacKenzie KJD, Smith ME Multinuclear Solid-State NMR of Inorganic Materials, Pergamon Materials Series

47. Skibsted J, Jakobsen HJ, Hall C (1995) Quantification of calcium silicate phases in Portland cements by 29Si MAS NMR spectroscopy. Journal of the Chemical Society, Faraday Transactions 91:4423. https://doi.org/10.1039/ft9959104423

48. Cherney EA, Hooton RD (1987) Cement Growth Failure Mechanism in Porcelain Suspension Insulators. IEEE Transactions on Power Delivery 2:249–255. https://doi.org/10.1109/TPWRD.1987.4308096

49. Magi M, Lippmaa E, Samoson A, et al (1984) Solid-state high-resolution silicon-29 chemical shifts in silicates. The Journal of Physical Chemistry 88:1518–1522. https://doi.org/10.1021/j150652a015

50. Andersen MD, Jakobsen HJ, Skibsted J (2004) Characterization of white Portland cement hydration and the C-S-H structure in the presence of sodium aluminate by 27Al and 29Si MAS NMR spectroscopy. Cement and Concrete Research 34:857–868. https://doi.org/10.1016/j.cemconres.2003.10.009

51. Shoval S (1988) Mineralogical changes upon heating calcitic and dolomitic marl rocks. Thermochimica Acta 135:243–252. https://doi.org/10.1016/0040-6031(88)87393-3

52. Hughes DC, Jaglin D, Kozłowski R, Mucha D (2009) Roman cements — Belite cements calcined at low temperature. Cement and Concrete Research 39:77–89. https://doi.org/10.1016/j.cemconres.2008.11.010